

Wang et al., *Gli3* in the neurogenic SVZ establishment

## **Supplemental Information**

**Title: Gli3 repressor controls cell fates and cell adhesion for proper establishment of neurogenic niche**

**Hui Wang, Anna W. Kane, Cheol Lee, and Sohyun Ahn**

### **Inventory of Supplemental Material:**

**1. Supplemental Figures S1-S4 and corresponding Figure Legends**

**Figure S1 related to Figure 1**

**Figure S2 related to Figure 2**

**Figure S3 related to Figure 3**

**Figure S4 related to Figure 5**

**2. Supplemental Experimental Procedures**

**3. Supplemental References**

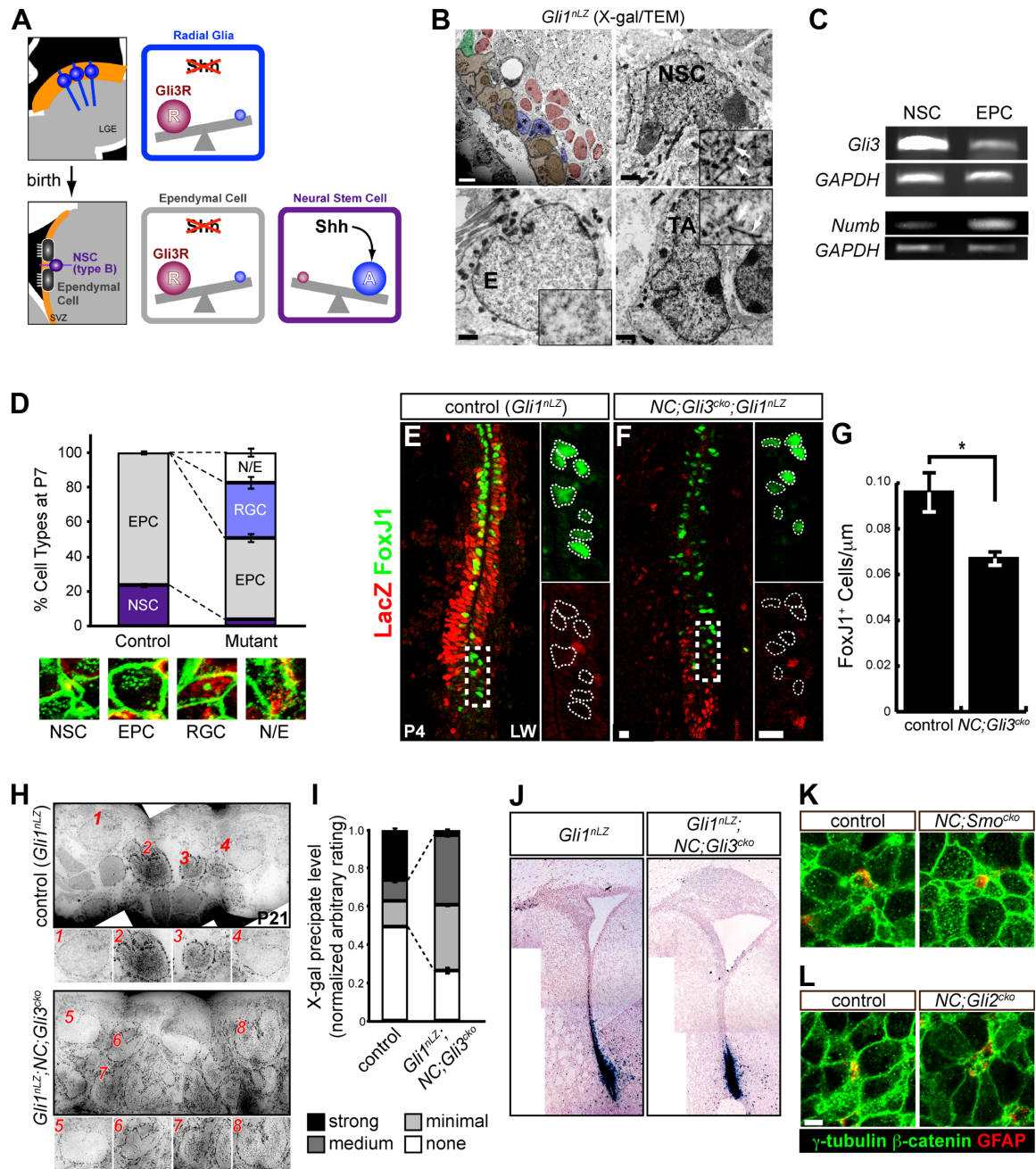


**Figure S1. Analysis of distinct VZ/SVZ cell populations in control and *NC;Gli3<sup>cko</sup>*, related to Figure 1.**

(A) Model for distribution of Gli3 Repressor (Gli3R) and Gli activators in response to Shh signaling is shown for embryonic radial glia and postnatal ependymal cells and neural stem cells. Before birth, Shh signaling is not active in developing lateral ganglionic eminence (LGE) resulting in more abundant presence of repressor than activator. After birth, ependymal cells retain the balance of repressor and activator as in radial glia. In contrast, NSCs respond to Shh signaling and Gli3R level becomes negligent.

**(B)** In adult SVZ, only neural stem cells (NSCs) and transit-amplifying (TA) cells respond to Shh signaling and express *Gli1* as analyzed in *Gli1<sup>nLZ</sup>* mice. This suggests Gli3 protein exists as an activator in NSCs and TA cells, while as a repressor in other cell types if it is expressed. White arrows in the inset images indicate nuclear X-gal precipitates (black elongated spikes). Scale bars, 5  $\mu\text{m}$  (white) and 1  $\mu\text{m}$  (black).

**(C)** RT-PCR result shows that *Gli3* and *Numb* are expressed in both NSCs and ependymal cells (EPC), but at differential levels. *GAPDH* is input control.

**(D)** Cell types were quantified in P7 lateral wall whole mount in *NC;Gli3<sup>cko</sup>* mutants and controls. NSCs were small with GFAP expression confined to the center of a pinwheel. EPCs were larger, cuboid cells with numerous  $\gamma$ -tubulin+ basal bodies but without GFAP expression. RGCs were identified as cuboid cells with a single basal body and GFAP expression, and N/E were any cells with mixed fate, expressing GFAP while having an ependymal shape and multiple basal bodies. Only EPCs and NSCs were identified in the control while the mutant contained fewer EPCs and NSCs, and more RGCs and N/E type cells.

**(E-G)** FoxJ1 expression is reduced at P4. Immunohistochemistry of FoxJ1 (green) and LacZ (red) staining in control *Gli1<sup>nLZ</sup>* (E) and *NC;Gli3<sup>cko</sup>;Gli1<sup>nLZ</sup>* SVZ (F) at P4. *NC;Gli3<sup>cko</sup>* (F) shows fewer FoxJ1+ cells than the control (E) and number of FoxJ1+ cells were quantified (G, \* indicates  $p < .05$ ). LacZ (red) staining indicates *Gli1* expressing cells. There were fewer LacZ+ cells in the *NC;Gli3<sup>cko</sup>;Gli1<sup>nLZ</sup>* mutant SVZ (F) as compared to the control (E). Scale bar, 10 $\mu\text{m}$ .

**(H)** The level of *Gli1* expression (Shh responsiveness) was analyzed at the ultrastructural level in control and *NC;Gli3<sup>cko</sup>* SVZ at P21. Transmission electron microscopic (TEM) study indicates that there is a clear difference in levels of X-gal precipitates in nuclei of SVZ cells in the control. For example, cells numbered 1 and 4 (ependymal cells) show no nuclear X-gal precipitates while #2 cell (NSC) shows abundant X-gal precipitates and #3 cell (TA cell) with intermediate level. In contrast, such distinction between the level of X-gal precipitates is not observed in *NC;Gli3<sup>cko</sup>* in which the level of X-gal precipitates appear similar across numerous cells (#6, 7, and 8 show intermediate levels of X-gal precipitates).

**(I)** The level of X-gal precipitates in individual cell was categorized into four groups (strong, medium, minimal and none) in a blind manner and quantified.

**(J)** X-gal staining for nuclear LacZ (nLZ) in P4 coronal sections. Shh signaling activation was assessed by nLZ expression in *Gli1<sup>nLZ</sup>*. *Gli1* expression is not increased in the *NC;Gli3<sup>cko</sup>* mutants indicating that there is no ectopic increase in Shh signaling activation in the absence of *Gli3*

**(K)** Immunohistochemistry for  $\beta$ -catenin/ $\gamma$ -tubulin (green) and GFAP (red) in P7 lateral wall whole mounts show that cells with mixed identity were not found in P7 *NC;Smo<sup>cko</sup>* mutants nor their littermate controls. The niche organization was also maintained in the *NC;Smo<sup>cko</sup>* mutants. Cell identity and niche organization were also normal in the *NC;Gli2<sup>cko</sup>* mutants at P7. Scale bar, 10 $\mu\text{m}$ .

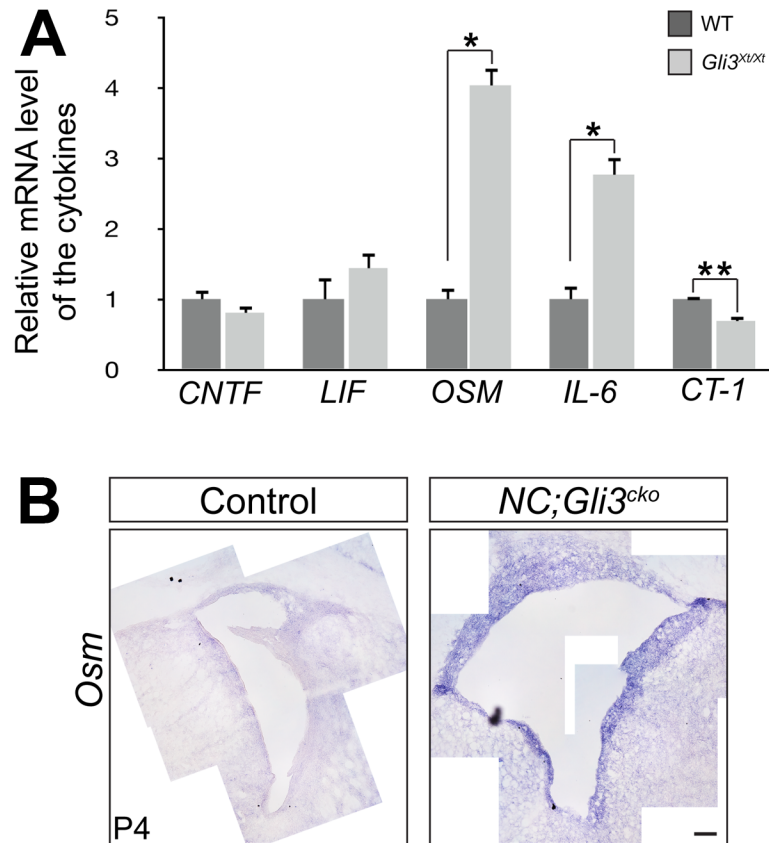


**Figure S2. mRNA level of IL-6 family signals in wild type and *Gli3* mutants, related to Figure 2**

**(A)** At E16.5, *Osm* and *IL-6* mRNA is increased in *Gli3<sup>Xi/Xi</sup>* compared to wild type. *CT-1* mRNA is decreased in the mutants. *CNTF* and *LIF* mRNA is not changed. \*,  $p < 0.05$ . \*\*,  $p = 0.002$ .

**(B)** *Osm* mRNA is increased in *NC;Gli3<sup>cko</sup>* SVZ compared to control at P4. Scale bar, 5mm.



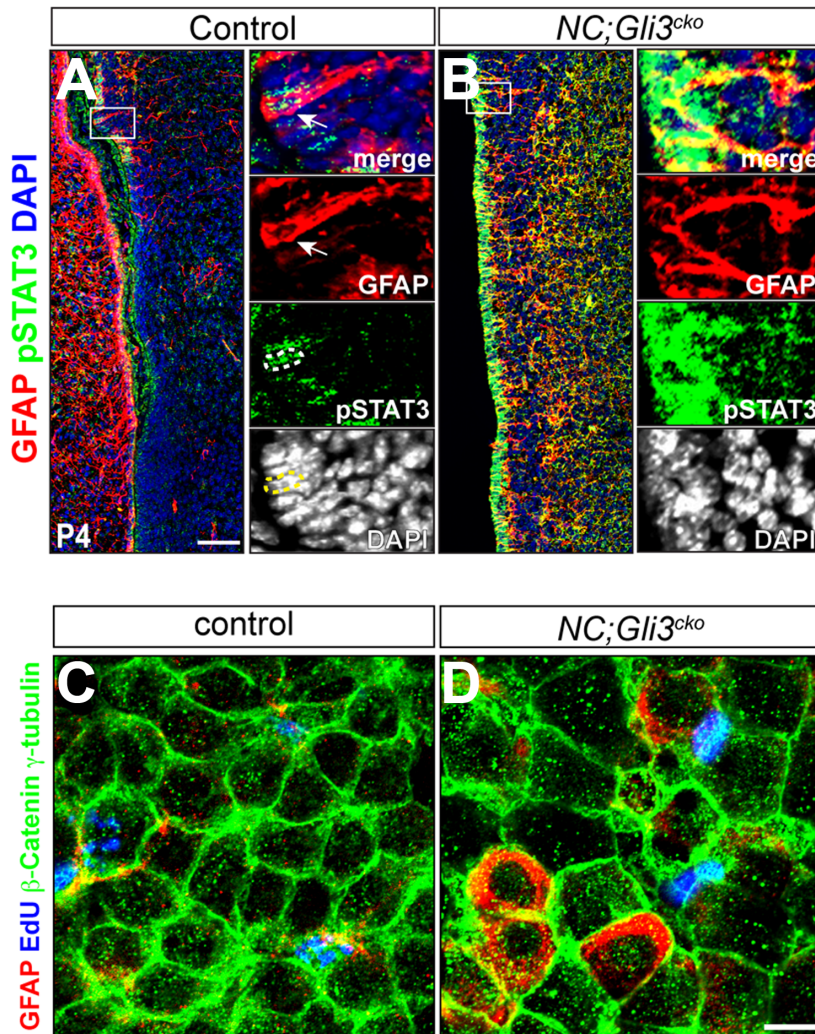


**Figure S3. Overactivation of STAT3 and absence of proliferation in *Gli3* mutants, related to Figure 3.**

**(A and B)** Overactivation of STAT3 in *NC;Gli3<sup>cko</sup>* SVZ at P4.

Immunohistochemistry of pSTAT3 and GFAP in control and *NC;Gli3<sup>cko</sup>* SVZ at P4. Both pSTAT3 (green) and GFAP (red) are upregulated in *NC;Gli3<sup>cko</sup>* (B) compared to control (A). Higher magnification images of boxed areas are shown in right panels. A cell coexpresses pSTAT3 and GFAP is indicated by an arrow. Nucleus of the same cell is outlined by dashed circle. Scale bar, 50  $\mu$ m.

**(C and D)** Mutant cells in *NC;Gli3<sup>cko</sup>* carrying both NSC and ependymal characteristics (GFAP+ multi-ciliated cells) do not proliferate. 76 such mutant cells were analyzed and none of them showed EdU (blue) incorporation. Scale bar, 50  $\mu$ m.

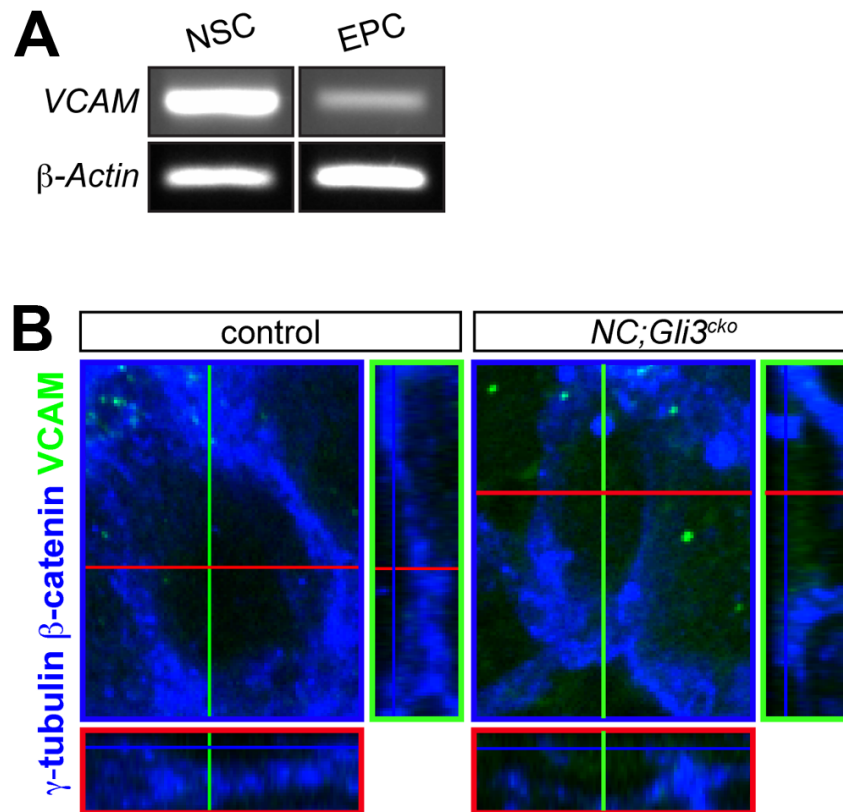


**Figure S4. mRNA expression of *VCAM* in NSCs and EPCs and *VCAM* distribution in mutant cells, related to Figure 5.**

(A) qRT-PCR result shows that *VCAM* is expressed in both NSCs and EPCs but at differential levels in the adults (8.87 folds higher in NSCs).  *$\beta$ -actin* is an input control. (B) *VCAM* is distributed throughout mutant cells. Immunohistochemistry was performed for  $\beta$ -catenin (blue) and *VCAM* (green) in P21 lateral wall whole mounts. Orthogonal views through one representative cell for *NC;Gli3<sup>cko</sup>* mutant and control show that *VCAM* staining is diffuse throughout the cell in the *NC;Gli3<sup>cko</sup>* mutant, while confined to the surface and NSC-EPC boundary in the control.

## Supplemental Experimental Procedures

**Mice and DNA constructs.** All mice were handled according to the guideline of the Institutional Animal Care and Use Committee of NIH. *Nestin-Cre* (Tronche et al., 1999), *Gli3<sup>F/+</sup>* (Blaess et al., 2008), *Gli3<sup>Xtl/+</sup>* (Hui and Joyner, 1993), *Gli1<sup>CreER/+</sup>* (Ahn and Joyner, 2004), *FoxJ1-Cre* (Zhang et al., 2007), *GFAP-GFP* (Zhuo et al., 1997), and *R26<sup>R/+</sup>* (Soriano, 1999), *R26<sup>tdTomato/+</sup>* (Madisen et al., 2010) mice were genotyped as described previously. *NC;Gli3<sup>Xtl/+</sup>* was crossed with *Gli3<sup>F/F</sup>* to generate *NC;Gli3<sup>cko</sup>* conditional mutants. DNA plasmids used for electroporation were RFP and Cre (Wang et al., 2011).

**Immunohistochemistry, TEM, histology and brain analyses.** Fluorescent immunostaining on sections was performed as described (Ahn and Joyner, 2004). Briefly, mice were deeply anesthetized and transcardially perfused with PBS and 4% paraformaldehyde/PBS. Dissected brains were fixed in 4% paraformaldehyde/PBS and were either cryoprotected in a sucrose gradient for embedding in OCT to obtain frozen sections or sectioned with a vibratome (Leica VT1000) for free floating sections. Dissection and processing of the whole mount SVZ on the lateral wall of the lateral ventricles followed the Alvarez-Buylla lab protocol (Mirzadeh et al., 2010; Mirzadeh et al., 2008). The primary antibodies and their dilution factors used were: rabbit antibodies against GFAP (1:1000, DakoCytomation),  $\beta$ -catenin (1:1000, Sigma), Numb (1:200, Novus), pSTAT3 (1:1000, Cell Signaling), LNX2 (1:200, Abgent) and  $\gamma$ -tubulin (1:1000, Sigma); mouse antibodies against  $\beta$ -catenin (1:1000, Sigma), FoxJ1 (1:250, eBiosciences), GFAP (1:500, Chemicon), and  $\gamma$ -tubulin (1:1000, Abcam), E-Cadherin (1:200, BD Transduction); chicken antibody against RFP (1:1000, Rockland); Rat antibody against VCAM (1:100, BD Transduction). The secondary antibodies used were species-specific antibodies conjugated with Alexa Fluorophores 488, 555, or 633 (1:500, Invitrogen). Antigen retrieval was performed using the EMS Retriever (EMS 62700-10) using Buffer A (EMS 62706-10) for FoxJ1 staining. Images were taken with a Leica DM6000B microscope equipped with a Hamamatsu ORCA-AG digital camera or with LSM510 inverted confocal microscope. Images were processed with Volocity, LSM510, or Adobe Photoshop CS4.

For X-gal TEM, the animals were perfused with 0.9% saline followed by 100 ml

of 4% paraformaldehyde and 0.5% glutaraldehyde in PBS (Wichterle et al., 1999). For regular TEM, the animals were perfused with 4% PFA with 2.5% glutaraldehyde in 0.1 M sodium cacodylate buffer, pH 7.4. Fixed brain was cut coronally at 100  $\mu$ m thickness using a vibratome and brain sections were either incubated in X-gal (5-Bromo-4-chloro-3-indolyl  $\beta$ -D-galactoside) solution at 37 °C overnight or just rinsed in 0.1 M sodium cacodylate buffer. Sections were further postfixed in 1% osmium tetroxide in 0.1 M sodium cacodylate buffer, serially dehydrated in ethanol, infiltrated with 812 resin/ethanol, and polymerized in 100 % resin for 16 hours at 60 °C. Thin sections were cut at 50 nm thicknesses on a Reichert-Jung Ultracut-E ultramicrotome and collected on 30 nm thick LuxFilm grids (Ted Pella, Inc.). The grids were post-stained with uranyl acetate and lead citrate and imaged with a JEOL 1010 transmission electron microscope operating at 80 kV. Cell types of the SVZ were identified according to criteria described in (Doetsch et al., 1997).

**Western analysis.** Western analysis for gp130, Numb, LNX2 and GAPDH was performed as described (Dho et al., 1999). Briefly, brain extracts were separated on a 7.5% SDS-PAGE gel under reducing conditions and transferred onto PVDF (Bio-Rad) membrane. Membranes were blocked in 5 % BSA in TBS-T for 1hr and incubated at 4 °C overnight with rabbit anti-Numb (1:800, Abcam), rabbit anti-gp130 (1:200, SC Biotechnology), rabbit anti-LNX2 (1:200, Abgent) and rabbit anti-GAPDH (1:1000, Abcam). The results were captured and analyzed using ChemiDoc XRS+ (BioRad).

**FACS-isolation of neural stem cells and ependymal cells.** The SVZs of 2-3 months old *Gli1<sup>CreER/+</sup>;hGFAP-GFP;R26<sup>tdTomato/+</sup>* mice three weeks after tamoxifen treatments (2 administrations of 10 mg separated by 24 hours) or *FoxJ1-Cre;R26<sup>YFP/+</sup>*, *FoxJ1-Cre;Gli3<sup>F/Xt</sup>;R26R*, *FoxJ1-Cre;Gli3<sup>F/+</sup>;R26R*, *hGFAP-Cre;Gli3<sup>F/Xt</sup>;R26R*, or *hGFAP-Cre;Gli3<sup>F/+</sup>;R26R* mice were microdissected and dissociated using papain (Worthington Biochemicals, NJ). The cell suspension was triturated and filtered through a 40  $\mu$ m cell strainer and myelin was removed by Myelin Removal Beads (Milteny Biotech, CA). For measuring the Cre efficiency, dissociated cells were loaded with fluorescein di-b-D-galactoside (FDG) by osmotic shock as described in Mukoyama et al. (2002). Cells were sorted for GFP and/or tdTomato expression or FDG loading using a MoFlo cell

sorter (Beckman Coulter). Dead cells were excluded by 7-AAD (Invitrogen, CA) staining and gates for collection were set using cells from wild type mice as a negative control.

**qRT-PCR.** Total RNA was isolated from freshly dissected tissue or FACS-isolated cells using Trizol reagent (Invitrogen), treated with DNase-I (Roche) and further cleaned using spin columns (Qiagen). Equal quantities (100 ng) of total RNA were then reverse transcribed to obtain cDNA by using iScript kit (BioRad). Reverse transcription PCR was performed with a 5 minutes denaturation at 95 °C followed by 35 cycles of denaturation for 30 seconds at 95 °C, annealing for 30 seconds at 58 °C (*Numb* and others) or 30 seconds at 56 °C (*GAPDH*), and extension for 30 seconds at 72 °C, and final extension for 7 minutes at 72 °C. Real-time quantitative PCR was performed using SYBR Green Mastermix (Roche) in a LightCycler 480 II instrument (Roche). *GAPDH* reaction was run in parallel with other test genes to normalize the gene expression. Samples were replicated three times for each run and experiments were repeated twice. Primers used are as following: *Numb-F*, 5'-GAGAGCATCAGCTCCTTGTG-3'; *Numb-R*, 5'-GAGGAGAAGGGGTCCTCAG-3'; *GAPDH-F*, 5'-tgacatcaagaaggtggtgaagc-3'; *GAPDH-R*, 5'-CCCTGTTGCTGTAGCCGTATTC-3'; *Gli3-F*, 5'-AGCAAGCCCACAAGCGAGT-3'; *Gli3-R*, 5'-GCTTCTCCCCAGTGTGTCTT-3';  $\beta$ -*Actin-F*, 5'-GTGGGCCGCTCTAGGCACCA-3';  $\beta$ -*Actin-R*, 5'-CGGTTGGCCTTAGGGTTCAGG-3'. Primers of *Il6st*, *CNTF*, *LIF*, *OSM*, *IL-6*, *CT-1*, *CNTFR*, *LIFR*, *OSMR*, *IL-6R* and *VCAM* were obtained from SABioscience qPCR Assay.

### **Supplemental References**

Madisen, L., Zwingman, T. A., Sunkin, S. M., Oh, S. W., *et al.* (2010). A robust and high-throughput Cre reporting and characterization system for the whole mouse brain. *Nat Neurosci* *13*, 133-40.

Mukoyama, Y.S., Shin, D., Britsch, S., Taniguchi, M., and Anderson, D.J. (2002). Sensory nerves determine the pattern of arterial differentiation and blood vessel branching in the skin. *Cell* *109*, 693-705.

Soriano, P. (1999) Generalized lacZ expression with the ROSA26 Cre reporter strain. *Nat Genet* *21*, 70-71.